Dynamical Studies on the Dd Stau Catalyzed Fusion and Comparing Obtained Results by Muon

S.N. Hoseinimotlagh
Department of Physics, Shiraz branch Islamic Azad University, Shiraz, Iran
M. Ghasemi Shabankareh
Imam Hossein Comprehensive University, Faculty and Research Institute of Fundamental Science, Physics Department, Tehran, Iran
S. Kianafraz
Department of Physics, Payam Noor University, Mashhad, Iran

Abstract

In this paper, we use of a new way for nuclear fusion, called Stau Catalyzed Fusion (SCF). Stau particle is superpartner of Tau lepton, that can be catalyzed fusion fuel atoms and lead to the fusion between them. By presenting the network of dd Stau catalyzed fusion and writing the dynamical point kinetic equations on it and then solving them in available conditions we calculated the stau catalyzed cycling rate and finally compare obtained results by the dd Muon Catalyzed Fusion(MCF) . We hope that Stau catalyzed fusion become economical method to produce energy in the future.
**Keywords:** Stau, Muon, Fusion, Deuterium, Dynamics.

1. Introduction

Nuclear fusion played and still plays an important role in the Universe. About 1 million years after the big bang large amounts of 4He were created by the fusion of protons on a global scale, and later on until now heavier elements were and are created in the huge fusion reactors provided by the interior of the stars. On earth, the concepts envisaged for a fusion reactor are muon catalyzed *cold fusion*, *thermonuclear fusion* by magnetic plasma confinement in tokamaks or stellarators, and finally laser- or beam-induced *inertial fusion*. In this paper we shall concentrate on muon catalyzed *cold fusion and a new form of cold fusion that is called Stau catalyzed fusion* .In magnetic field confinement fusion, a magnetic field is used to confine a plasma of completely free electrons and nuclei, and the plasma is allowed to reach ultrahigh temperatures. In the other method, called 'inertial confinement fusion', a laser beam is used to rapidly compress the fuel into a superdense state (1,000 times denser than a solid). In both cases, very large facilities are required to achieve the ultrahigh temperatures or superdense states necessary to induce nuclear fusion. In contrast, muon-based nuclear fusion does not require such ultrahigh temperatures or superdense states. Compared to magnetic field confinement fusion and inertial confinement fusion, muon-base nuclear fusion could allow stable nuclear fusion to be induced in a smaller facility at lower cost for a longer period of time. What kind of particle is a muon? Mesons are produced by collisions between atomic nuclei in the atmosphere and protons arriving from space, and these mesons immediately decay into muons and neutrinos, which bombard the Earth continuously. Muons can now be created artificially using an accelerator by directing a beam of high-speed protons at a suitable target material. In 1995, RIKEN established the

RIKEN–RAL Muon Facility at the Rutherford Appleton Laboratory in the United Kingdom . The RIKEN–RAL Muon Facility generates the most powerful pulsed muon beam in the world, and the center has taken a leading role in applied studies of muons. The muon belongs to the lepton group of elementary particles, which includes electrons. It has a lifetime of 2.2μs, and a mass one-ninth that of a proton and 207 times that of an electron. There are positively charged muons and negatively charged muons. In a material, the positive muon acts as a 'light' proton, while the negative muon acts as a 'heavy' electron. Muon-based nuclear fusion is conducted using negative muons. In dd muon catalyzed fusion a gas of deuterium is cooled to temperatures below around −250°C, causing the gas to form a liquid or solid. The injection of a beam of muons (μ) into the medium then generates muonic deuterium atoms (dμ), which are similar to hydrogen atoms. As muons are 207 times heavier than electrons, the muon orbits the nucleus at a distance much shorter than that for electrons. Thus, dμ atoms are extremely small, and because the dμ atoms have no charge, they collide with deuterium atoms without being affected by repulsive electrical force. This process produces muonic deuterium–deuterium molecules (ddμ), which are also similar to hydrogen atoms, and which have a nucleus consisting of a muon, and two deuterium nucleus. Similar to the dμ atom, the ddμ molecule is extremely small, which allows the deuterium nuclei to come into very close proximity, thus inducing d–d nuclear fusion .After the occurrence of d–d nuclear fusion, the muon in the dd molecule is liberated and becomes available for the creation of a new ddμ molecule. Thus a chain of nuclear fusions occurs. This reaction is called 'muon-catalyzed nuclear fusion' because the muons act like a catalyst that drives nuclear fusion. About 1% of the liberated muons, however, become stuck to produced nuclei. If in the above discussion , only Stau particle replaced by muon it produce new approach for cold fusion that is called Stau catalyzed d-d fusion.(Fig.1)

Figure-1. Mechanism of atoms and molecules formation in Stau catalyzed fusion
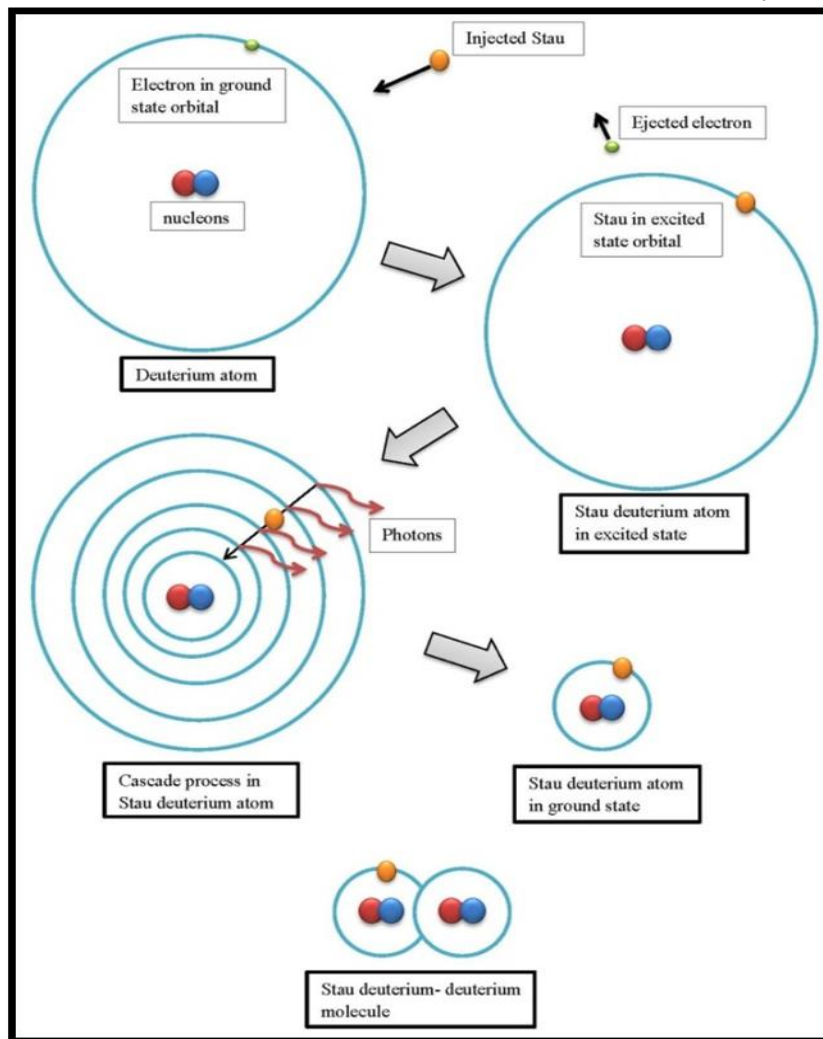
2. Supersymmetric Standard Model

In fact ,Supersymmetry , is one of the most interesting topics beyond the standard model. This theory involves not only problems of the standard model, but also paved the way for us to describe the density of dark matter in the universe. One of the most important models in this theory is the MSSM model (Aitchison, 2007), (Porod, 1998) and (Martin, 2008). Various particles predicted in this model, one of them has been identified as the Stau. For further reading on the supersymmetric standard model and issues related to them, you can see the references (Hamaguchi, *et al.*, 2012) and (Hosseinimotlagh and Shamsi, 2008).In Table.1, the general category of supersymmetric particles are given.

Table-1. The general category of supersymmetric particles (the numbers in this table may be different in different sources but all sources are the same type of particles) (Eidelman, et *al.*, 2004)

Sfermions		Lower mass bound (GeV)	Bosinos		Lower mass bound (GeV)
$\tilde{u}$	u −Squark	250	$\tilde{g}$	Gluino	300 ($m_{\tilde{q}} = M_{\tilde{g}}$)
$\tilde{d}$	d −Squark	-do-			195 (otherwise)
$\tilde{c}$	c −Squark	-do-	$\tilde{\chi}_1^0$	lightest Neutralino	59 (mSUGRA)
$\tilde{s}$	s −Squark	-do-			40 (otherwise)
$\tilde{t}$	Stop	135 ($\tilde{t}_1$)	$\tilde{\chi}_2^0$	next lightest Neutralino	62.4
$\tilde{b}$	Sbotton	91 ($\tilde{b}_1$)	$\tilde{\chi}_3^0$	second heaviest Neutralino	99.9
$\tilde{e}$	Selectron	99 ($\tilde{e}_R$)	$\tilde{\chi}_4^0$	heaviest Neutralino	-do-
$\tilde{\upsilon}_e$	e −Sneutrino	45	$\tilde{\chi}_1^\pm$	lighter Chargino	103 (gauginolike)
$\tilde{\mu}$	Smuon	95 ($\tilde{\mu}_R$)			99 (higgsinolike)
$\tilde{\upsilon}_\mu$	Muon-Sneutrino	45	$\tilde{\chi}_2^\pm$	heavier Chargino	-do-
$\tilde{\tau}$	Stau	80 ($\tilde{\tau}_1$)	$\tilde{G}$	Gravitino	1.0×10^{-14}
$\tilde{\upsilon}_\tau$	Tau-Sneutrino	45			

In fact ,MSSM model is the first extension of the standard model to the supersymmetry theory. Strong interacting between the superpartners namely Gluinos and Squarks with masses less than $2.5\ TeV$ in the Large Hadron Collider or LHC for short, is a significant discovery. Physicists at the LHC have started this project from 2008. Among the supersymmetric particles, the lightest particle (LSP) plays the essential role and in cosmology as one of the main candidates for dark matter is considered. In the LHC, the signal of supersymmetric particles is dependent on the nature of the lightest particle. Lightest supersymmetric particle is probably that a Neutralino $\tilde{\chi}_1^0$ which escape from the detector and its effects as a missing energy E_T leaves. Another possibility for the lightest particle is Gravitino $\tilde{G}$ that is in fact a superpartner of graviton in the standard model. Gravitino are paired in a very small sector of the MSSM with other supersymmetric particles. Namely proportional to $\dfrac{1}{M_{pl}}$

[7].The next lightest supersymmetric particle (NLSP) which necessarily its decay contains the Gravitino due to the small sector has a long lifetime. The most obvious candidate for the next lightest charged supersymmetric particle (CNLSP) is scalar Stau in the Staus groups which we show it with $\tilde{\tau}_1$ and it is significantly lighter than other sleptons. It should be noted that the group include S. It should be noted that the group of Stau is a one type of particles with different mass because Stau mass

is dependent on Gravitino mass and energy production, and Gravitino mass and energy production are variable (Heckman, *et al*., 2010), (Pradler, 2009), (Hamaguchi, *et al*., 2006), (Buchmuller, *et al*., 2004a) and (Buchmuller, *et al*., 2004b).The charged particle leaves the tracts in the central detector (ATLAS and CMS), given additional information for the SUSY particle reconstructions. If the NLSP decays in the main detector, a display vertex may be observed as well. Expected lifetime for CNLSP is without limitations because their lifetime is dependent on Gravitino mass squared that is still unknown (Heckman, *et al*., 2010), (Pradler, 2009), (Hamaguchi, *et al*., 2006), (Buchmuller, *et al*., 2004a) and (Buchmuller, *et al*., 2004b).On the other hand the gravitons mass with the total scale of supersymmetry breaking in the hidden area is proportional and therefore the goal of physics is to estimate the lifetime of supersymmetric particles. Calculating the lifetime of these particles gives us direct information about the hidden sector. It described the area is not our goal in this article And therefore for more study you first see references (Loff, *et al.*, 1981) and (Buchmuller, *et al.*, 2004b) and then for more details see references (Dreiner, *et al.*, 2010) and (Feng and Smith, 2005).

The decay of the main LHC detectors are effectively and efficiently if the decay length is significantly short, $\approx 10m \times N_{produced}$, where $N_{produced}$ is the number of produced supersymmetric particles. On the other hand, for a typical SUSY production cross section, a direct observation of the decay is very difficult for $\tau_{CNLSP} > 0.001 \sec$ .Of course there are ways to trap CNLSP in references (Brandenburg, *et al.*, 2005,) and (Hamaguchi, *et al.*, 2004) come. Also, to continue this discussion and the various ways in order to view and sort supersymmetric particles you can see references (Martin, 2008,) and (Porod, 1998).

But, our selective model in this paper for determining LSP and NLSP is minimal supergravity or mSUGRA. In this model, we assumed that the lightest super symmetric particle is Gravitino and the next lightest particle is scalar Stau ($\tilde{\tau}_1$) that is charged particle. It should be noted that the Stau group based on mass and other characteristics can be divided into two categories: $\tilde{\tau}_1$ and $\tilde{\tau}_2$ .This model assumes that the R- parity is conserved and this is the cause of the NLSP will decay to Gravitino through very weak interactions suppressed by the Planck scale. Parity conservation is also an indication that the Gravitino is stable. So according to this model, We will study on Stau ($\tilde{\tau}_1$) to use it for nuclear fusion catalyst in this article (Heckman, *et al.*, 2010), (Pradler, 2009), (Hamaguchi, *et al.*, 2006), (Roeck, *et al.*, 2005), (Delphi Collaboration, 2001) and (Panotopoulos, 2008).

Our desired model is mSUGRA, and in this model, the lightest particles are Gravitino and Stau, and we know that Stau particle must be decay to Gravitino but because of weak interactions in strongly finite Planck area , it has a long lifetime.

So by using the two body decay equation for decay Stau, we can calculate the Stau lifetime. Decay width of Stau to Gravitino and Tau can be written as (Pradler, 2009), (Hamaguchi, *et al.*, 2006), (Buchmuller, *et al.*, 2004a) and (Buchmuller, *et al.*, 2004b):

$$\Gamma_{\tilde{\tau}}^{2-body} (\tilde{\tau}_1 \rightarrow \tau + \tilde{G}) = \frac{\left(m_{\tilde{\tau}}^2 - m_{3/2}^2 - m_{\tau}^2\right)^4}{48\pi m_{3/2}^2 M_P^2 m_{\tilde{\tau}}^3} \left[1 - \frac{4m_{3/2}^2 m_{\tau}^2}{\left(m_{\tilde{\tau}}^2 - m_{3/2}^2 - m_{\tau}^2\right)^2}\right]^{\frac{3}{2}} \left(\frac{GeV}{c^2}\right)^2 \quad (1)$$

where $m_{\tilde{\tau}}$, $m_{3/2}$ and m_{τ} are mass of Stau, Gravitino and Tau respectively. M_p is reduced plank mass such that:

$$M_p = \left(8\pi G_N\right)^{-1/2} \quad (2)$$

and G_N is gravitational constant:

$$G_N = 6.70881 \times 10^{-39} \hbar c \qquad \left(\frac{GeV}{c^2}\right)^{-2} \quad (3)$$

then

$$M_P^2 = (8\pi G_N)^{-1} = \frac{(2.435328254 \times 10^{18})^2}{\hbar c} \qquad \left(\frac{GeV}{c^2}\right)^2 \tag{4}$$

Now, for transform scale to time, equation (1) multiplied in $1/\hbar^2 c$, then

$$\Gamma_{\tilde{\tau}}^{2-body} = \frac{(m_{\tilde{\tau}}^2 - m_{3/2}^2 - m_\tau^2)^4}{48\pi m_{3/2}^2 M_P^2 m_{\tilde{\tau}}^3} \left[1 - \frac{4m_{3/2}^2 m_\tau^2}{(m_{\tilde{\tau}}^2 - m_{3/2}^2 - m_\tau^2)^2} \right]^{\frac{3}{2}} \times \frac{1}{\hbar^2 c} \qquad (s^{-1}) \tag{5}$$

Finally, Stau lifetime's is given by the following equation:

$$\tau_{\tilde{\tau}_1} = \frac{1}{\Gamma} = \frac{1}{\dfrac{(m_{\tilde{\tau}}^2 - m_{3/2}^2 - m_\tau^2)^4}{48\pi m_{3/2}^2 M_P^2 m_{\tilde{\tau}}^3} \left[1 - \dfrac{4m_{3/2}^2 m_\tau^2}{(m_{\tilde{\tau}}^2 - m_{3/2}^2 - m_\tau^2)^2} \right]^{\frac{3}{2}} \times \dfrac{1}{\hbar^2 c}} \qquad (s) \tag{6}$$

We calculated the numerical values of Stau lifetime for different values of $m_{\tilde{\tau}}$, $m_{3/2}$ and m_τ and therefore our obtained results are given in the Figure. 2 and Table. 2

As we know that, with decay of produced Stau particle a lot of energy is released in the form of kinetic energy of Gravitino and Tau. Tau kinetic energy (E_τ) can be calculated from the following relation (Pradler, 2009):

$$E_\tau = \frac{m_{\tilde{\tau}_1}^2 - m_{\tilde{G}}^2 + m_\tau^2}{2m_{\tilde{\tau}_1}} \tag{7}$$

Figure-2. logarithmic Stau lifetime diagram in terms of mass variations of gravitons and Stau. a) in the mass intervals $10^{-3} \le m_G \le 10^3 (GeV), 80 \le m_\tau \le 10^3 (GeV)$ b) $10 \le m_G \le 75 (GeV), 80 \le m_\tau \le 200 (GeV)$,

a)   **b)**
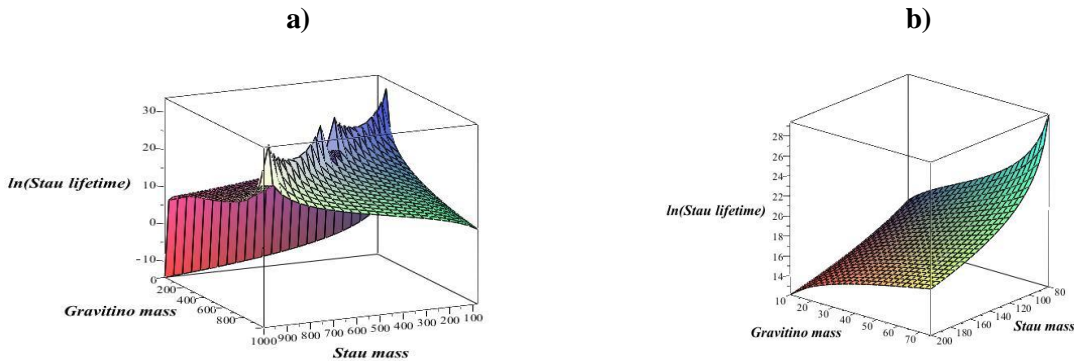

Table-2. Numerical values of Stau lifetime for different values of $m_{\tilde{\tau}}$, $m_{3/2}$ and m_τ.

	$\tau_{\tilde{\tau}_1}$ sec	$\tau_{\tilde{\tau}}$ years	$m_{\tilde{\tau}}$ GeV/c^2	$m_{3/2}$ GeV/c^2	m_τ GeV/c^2
1	$7.752466734 \times 10^{-7}$	few	150	0.00001	1.78
2	77.52480526	few	150	0.1	1.78
3	1.378993139×10^8	4.372758558	150	75	1.78
4	2.776233891×10^7	0.8803379922	100	20	1.78

Since for Stau catalyzed nuclear fusion, the long lifetime of Stau is very important, therefore, the best choices for us are cases 3 and 4 in Table 2. But the energy needed to produce case 3 is more than case 4, therefore we are use Stau with $m_{\tilde{\tau}} = 100$ GeV/c^2 and $\tau_{\tilde{\tau}} = 2.776233891 \times 10^7 s$ in our work.

3. Stau Production

One way to generate Stau-particle is scattering reaction between fixed target of nucleons and a Muon ($\mu + N\,(nucleon)$) [17]. Stau production cross section is dependent on the SUSY particle spectrum. Suppose that the production cross section of sleptons is $O\,(1)\,fb$ ([9]), and Muon energy has been fired toward the target in the lab frame is about $E_\mu = 1000\,TeV$. Since almost all SUSY particles decay rapidly to Stau, therefore the Stau production cross section is $O\,(1)\,fb$.

Now, with assuming " Fe " target with $O\,(1)\,Km$ length and $n_N = 5 \times 10^{24}\,cm^{-3}$ nucleons density, then the number of produced Stau per Muon is given by :

$$n_{\tau \approx} \sigma \times n_N \times 10^3$$
$$\approx 10^{-8} \tag{8}$$

The reader should be notice that the stopping range of the Muon inside the Fe target is $O\,(1)\,Km$ for $E_\mu = 1000\,TeV$ (Delphi Collaboration, 2001) and (Alexander, *et al.*, 1990). By using equation (8), we conclude that the energy required to produce one Stau is:

$$E_{\tilde\tau} = 10^8 \times 1000\,TeV = 10^{17}\,MeV \tag{9}$$

Also, there are the other methods for Stau production for instance the use of linear accelerators that produce Stau by using the electron – electron collision. The details about these methods in references (Dreiner, *et al.*, 2010) and (Feng. and Smith, 2005) are discussed. All these methods also need to have high energy.

4. Deuterium – Deuterium Stau Catalyzed Fusion Cycle

In Table3 we list three major branches of fusion reactions of deuterium atoms. For each reaction in this Table , Q-value is given.

Table-3. Three major branches of deuterium atoms nuclear reaction

i	Reaction branch	$Q\ \ (MeV\,)$
1	$d + d \to {}^3He + n$	3.1446
2	$d + d \to t + p$	3.9015
3	$d + d \to {}^4He + \gamma$	23.0710

When a Stau particle is sent to a chamber contained of deuterium atoms with liquid hydrogen density $N_d = 4.25 \times 10^{22}\,atoms/cm^3$ the following steps are occurred (see Fig.1)

In the first step , the trapped Stau absorbed by the nuclei of deuterium due to electromagnetic interactions between them, then the electron of the deuterium atom is ejected and replace with stau particle ,this process is called Stau atomic deuterium formation. Since the stau particle is very massive and larger than electron the radius of the Stau atomic deuterium is very shorter than deuterium .Notice that ,first Stau atomic deuterium in the excited state is formed and then by a cascade process, the atom is transited to ground state. Large mass of this particle causes severe shrink the atomic radius, and it brings about $15 fm$, according to Bohr's famous relations:

$$E_B = \frac{M}{8n^2}\left(\frac{e^2}{\varepsilon_0 hc}\right)^2 \quad (KeV\,) \tag{10}$$

$$a_{B\,(Stau)} = \frac{e}{8\pi\varepsilon_0 E_B} \quad (fm\,) \tag{11}$$

This process is similar to muon catalyzed fusion ,therefore to have a comparison between them ,the numerical values of Bohr's radius and binding energy for $\tilde{\tau}d$, μd and deuterium atoms are given in the Table.4. This mechanism ,causes that the Stau atom formed in second step acts similar to neutral particle and then can be trapped another deuteron with omitting Coulomb barrier between them and formed the Stau d-d molecule ($\tilde{\tau}dd$). Under these conditions, the distance between deuterium nuclei is become of $50fm$ or less and so the probability of fusion between deuterons significantly increases.

**Table-4.** Bohr's radius for Stau, Muonic and typical deuterium atoms

	$\tilde{\tau}d$	μd	d
$a_B(m)$	1.468×10^{-14}	2.703×10^{-13}	5.293×10^{-11}
$E_B(eV)$	4.902×10^4	2.663×10^3	13.601

In Figure .3 the comprehensive network of dd reaction by Stau catalyzed fusion is given. Due to the high lifetime of Stau, each Stau can be fused about of 10^{11} fusion reactions in its lifetime by repeating this cycle, and in each fusion cycle about 3 to 4 MeV energy is produced, thus the approximate energy produced per Stau is of order 3×10^{11} or 4×10^{11} .According to the Figure .3 the atomic and molecular formation rate of $\tilde{\tau}d$ and $\tilde{\tau}dd$ are $\lambda_a^{\tilde{\tau}d}$ and $\lambda_m^{\tilde{\tau}dd}$, respectively. In step three, the molecule $\tilde{\tau}dd$ is not stable and with the fusion rate of $\lambda_1^f, \lambda_2^f, \lambda_3^f$ decays to three different channels,

Channel 1- $^2H(d,n)^3H$

Chanel 2: $^2H(d,p)^3H$

Channel 3 : $^2H(d,\gamma)^4He$
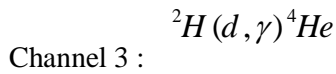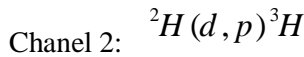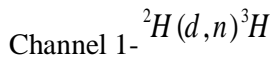
In each channel two cases are observed ,Case1) the Stau particle is free to perform another nuclear fusion. Case2) the Stau particle stuck to the charged particle $(p,t,^3He,^4He)$ and do not perform the other fusion reactions. These sticking probabilities in each channels are shown with p_s^1, p_s^2, p_s^3 , respectively '

In case 2), the Stau is out of the cycle of fusion and energy gain come down.

Figure-3. deuterium – deuterium fusion fuel cycle with Stau catalyst
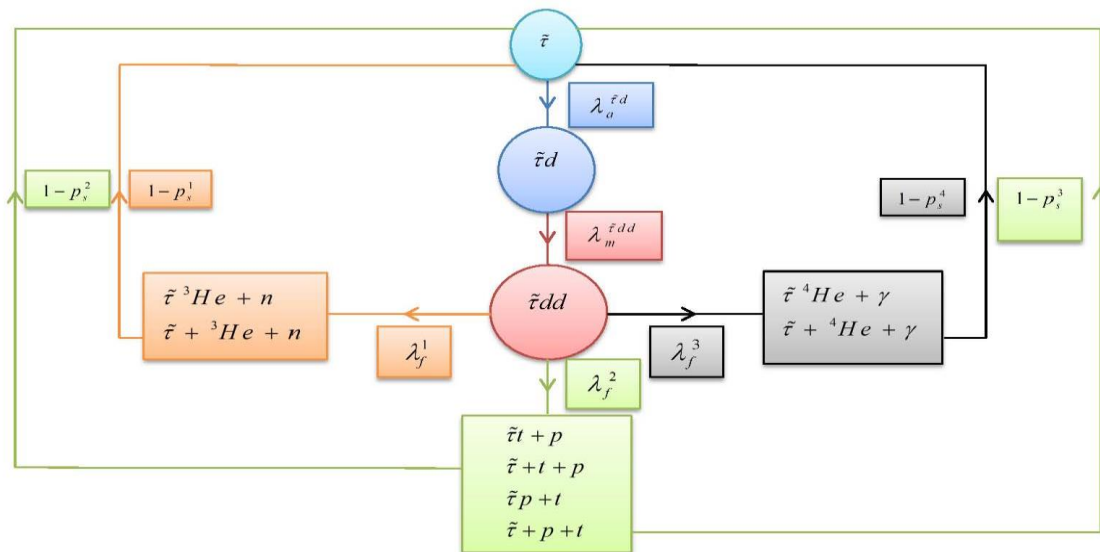
5. Stau Atomic and Molecular Formation Rate

In this section we calculate   the atom and molecule formation rate for Stau and similarly for Muon. Formation of atoms and molecules are performed by the following reactions:

$$\tilde{\tau} + d \xrightarrow{\lambda_a^{\tilde{\tau}d}} \tilde{\tau}d + e^-$$

$$\tilde{\tau}d + d \xrightarrow{\lambda_m^{\tilde{\tau}dd}} \tilde{\tau}dd \qquad (12)$$

$$\mu + d \xrightarrow{\lambda_a^{\mu d}} \mu d + e^-$$

$$\mu d + d \xrightarrow{\lambda_m^{\mu dd}} \mu dd \qquad (13)$$

We can see that from Figure. 3 , at first high energy Stau particle injected to a chamber of contains deuterium atoms , due to electromagnetic interactions , the electron of deuterium atom are separated from its and Stau is replaced with it ($\tilde{\tau}d$ formation mechanism in excited state) . Then it, during of the cascade process with photon emission transit to the ground state. Then $\tilde{\tau}d$ in ground state collides with other deuterium atoms to formed $\tilde{\tau}dd$ molecules. As we have known, similarly, these processes also occur for the Muon catalyzed fusion. Atoms and molecules formation rates depend on the following factors:

1- Energy and temperature: Formation of atoms or molecules are increased by increasing temperature and energy, since with increasing temperature the kinetic energy of the particles increases and therefore the effective collisions are increased for formation of atoms and molecules .

2- The mass of catalyst particle: With increasing mass of catalyst particle, formation rates of atoms and molecules are reduced, because the Stau atoms and molecules have the more mass respect to muonic atoms and molecules therefore they will move with slower velocity and hence the effective collision decreases. You can see this issue by comparing the numerical values of atoms and molecules formation rates for Stau and Muon that are presented in Table.5. Also, the formation rate of atoms differ from molecules because the molecules is heavier than atoms.

3- **Scattering cross section**: Increasing the scattering cross section leads to raising formation rates of atoms and molecules. You can see this issue by comparing the calculated values of formation rates of atoms and molecules for Stau or Muon that are presented in Table .5 .Since we assume a circular shape for cross section of Stau (Muon) atoms or molecules , therefore in this case , Bohr radius of lighter atoms or molecules in ground state is more than the radius of heavier atoms or molecules. Therefore , this point leads to the increasing the cross section atoms or molecules with less mass .

4- Fuel density: Density of fuel particles are highly effective direct relation with the formation rates of atoms and molecules. Because with increasing fuel density of the particles, the effective collision for formation of atoms and molecules have the catalyst increases.

We show that the formation rates of $\tilde{\tau}d$ and $\tilde{\tau}dd$ with $\lambda_a^{\tilde{\tau}d}$ and $\lambda_m^{\tilde{\tau}dd}$ respectively, and it can be calculated from the below equation

$$\lambda_{formation\ rate} = N_d \langle \sigma v \rangle \qquad (s^{-1}) \qquad (14)$$

assuming   that the particle collisions (e.g. Stau, Muon and deuterium) to the target leads to the production of catalytic atoms and molecules at different temperatures ,this issue become the cause of having different speeds in all possible directions, therefore Lambda is dependent on average of Sigmavee . Sigmavee average parameter is shown by $\langle \sigma v \rangle$ and are defined as follow ([1], [7], [28] and [5]):

$$\langle \sigma v \rangle = \frac{(8/\pi)^{1/2}}{M^{1/2}(kT)^{3/2}} \int_0^\infty \sigma E \exp(-E/kT)dE \qquad (m^3/s) \qquad (15)$$

then

$$\lambda_{formation\ rate} = N_a \frac{(8/\pi)^{1/2}}{M^{1/2}(kT)^{3/2}} \int_0^\infty \sigma E \exp(-E/kT)dE \qquad (s^{-1}) \qquad (16)$$

where, σ is scattering cross section on target. Now by inserting $\sigma \square \pi a_{B\,(electron)}^2$ and $\sigma \square \pi a_{B\,(catalyst\ particle)}^2$ inside the equation (16) and solving it we get the value of atom and molecular

formation rates, respectively. Here a_B is Bohr radius for electron, Stau or Muon in deuterium atom which presented in Table (4). Large difference between the formation rates of Stau molecules and Muon molecules are due to the large difference between Stau and Muon mass. Also, because the lifetime of the Stau is much more than Muon, the value of molecule formation rates parameter in Stau catalyzed fusion(SCF) is significantly less than the Muon catalyzed fusion(MCF), so that, if this parameter in our calculations changes about one or two order of magnitude (for example $10^3 \leq \lambda_{molecule\ formation} \leq 10^6$),then the Stau cycle efficiency and total energy production will not change the results significantly. But in the Muon catalyzed fusion variations of this parameter is very important. In the Table (5) value of atom and molecule formation rates at $T = 300K$ (room temperature) for SCF and MCF are calculated.

Table-5. Numericcal calculated values of atom and molecules formation rates for Stau and Muon catalyst

Atom and molecule formation for T = 300 K (sec^{-1})		
Stau catalyzed fusion	$\lambda_a^{\tilde{\imath}d}$	$\lambda_m^{\tilde{\imath}dd}$
	6.7062×10^{11}	5.1625×10^4
Muon catalyzed fusion	$\lambda_a^{\mu d}$	$\lambda_m^{\mu dd}$
	2.8771×10^{12}	2.4181×10^7

6. Sticking Probability

In SCF the probability of Stau stickiness to the charged particles produced by fusion reactions is most important parameter. This parameter is one of the most sensitive parameter in our work so that by any very small change in the order of magnitude, it leads to significantly change on the values of Stau cycle efficiency and energy gain. The effective of this parameter on the SCF is much more important than MCF, because the Stau production cost is higher than the Muon. Also due to high lifetime Stau compared to Muon, energy production per Stau is much more than Muon and so the Staus out of the fusion cycle, causing the loss of large amounts of energy compared to the Muon.

Sticking probability of Stau to the charged particles products of fusion is calculated as follows (Loff, *et al.*, 1981):

$$P_s \square \left(1 + \left(\frac{q_i a}{2}\right)^2\right)^{-4} \square \left(1 + \left(\frac{v_i/c}{4\alpha}\right)^2\right)^{-4} \tag{17}$$

where v_i is the velocity of the charged particle produced in nuclear fusion, a is the Bohr radius of the this atom. q_i is the momentum of charged particle. Now considering the Stau mass is much greater than other particles. We can neglect Stau momentum, and so the momentum of charged particles is calculated by the following relation:

$$q_i = \frac{c}{2m_i} \sqrt{\left(M^2 + m_i^2 - m_j^2\right)^2 - 4M^2 m_i^2} \tag{18}$$

Where M is the total mass of reactive particles. m_i and m_j are the mass of the particles produced in the reaction ($i = {}^3He, t, p, {}^4He$ and $j = p, n, \gamma$).

We calculated the sticking coefficients for different atoms of SCF and MCF and obtained results are given in Table (6) and (7).

Table- 6. Sticking coefficients for different atoms in Stau catalyzed fusion

			Sticking probability for Stau catalyzed fusion p_s^i				
Reaction Channels	i	Produced particle	p_s^i	$q\ (Kg\ m/s)$	$V_i\ (m/s)$	v_i/c	$E_K\ (MeV)$
${}^2H(d,n){}^3He$	1	${}^3He$	0.12399	3.50980×10^{-20}	7.24363×10^6	0.02416	0.79341

	-	n	------	3.50980×10^{-20}	2.16593×10^{7}	0.07224	2.37239
$^2H(d,p)^3H$	2	t	0.08630	3.89757×10^{-20}	8.04385×10^{6}	0.02683	0.97840
	3	p	0.00019	3.89757×10^{-20}	2.40723×10^{7}	0.08029	2.92800
$^2H(d,\gamma)^4He$	4	^4He	0.82992	1.22906×10^{-20}	1.91134×10^{6}	0.00637	0.73311
	-	γ	------	1.22906×10^{-20}	c	1.00000	22.99773

Table- 7. Sticking coefficients for different atoms in Muon catalyzed fusion

Sticking probability for Muon catalyzed fusion p_s^i				
Reaction	$^2H(d,n)^3He$	$^2H(d,p)^3H$		$^2H(d,\gamma)^4He$
i	1	2	3	4
Produced particles	^3He	t	p	^4He
Muon catalyzed fusion	0.0027	0.0027	0.0027	0.12

7. Fusion Rate

We used the approximately equation (19) for calculating fusion rate of each reaction branch. Since that in Stau catalyzed fusion, due to long lifetime of Stau and also much difference between the molecular formation rate ($\tilde{\tau}dd$) and fusion rate values, approximately calculations of numerical values of fusion rates, even up to three order of magnitude(for example $\lambda_f^1 \simeq 10^{14} \times 10^{\pm 3}$),significantly variations in Stau cycle efficiency and total energy production do not occur. In compared with Muon, because the Muon lifetimes is very short and so its lifetime comparable with molecule formation rates, therefore changes in the fusion rate of fusion reactions in MCF is salient. Fusion rates approximately are calculated from the following equation (Hosseinimotlagh and Shamsi, 2008):

$$\lambda \simeq \sigma(E) \times \bar{v} \times \frac{1}{\bar{V}} \qquad (s^{-1}) \qquad (19)$$

$\sigma(E)$ is the reaction cross section such that:

$$\sigma(E) = \frac{S(E)}{E} e^{-2\pi\eta} \qquad (20)$$

Where $\bar{E}$ and $\bar{v}$ are deuterium kinetic energy and speed respectively in the center of mass system. Using the uncertainty principle for $\bar{E}$ and $\bar{v}$ we have:

$$\bar{E} = 2\bar{E}_d = \frac{1}{m_d R^2} = \frac{\left(\frac{hc}{2\pi e}\right)^2}{m_d R^2} = 0.01069682121 \quad (MeV) \qquad (21)$$

$$M = m_0 m_1 / m_0 + m_1 = m_d / 2 \qquad (Mev/c^2) \qquad (22)$$

$$\bar{v} = \sqrt{\frac{\bar{E}}{2M}} = \sqrt{\frac{\bar{E}}{m_d}} = 0.004776235925 \qquad (\frac{m}{s}) \qquad (23)$$

Where $e^{-2\pi\eta}$ is the Gamow tunneling factor of the Coulomb barrier and η is the Sommerfeld parameter:

$$\eta = \frac{\alpha Z_0 Z_1}{\bar{v}} = 1.527845913 \qquad \left(\frac{m}{s}\right)^{-1} \qquad (24)$$

$$V = \frac{4}{3}\pi R^3 = 3.583412712 \times 10^{-40} \quad (m^3) \tag{25}$$

$S(E)$ is a spectroscopic factor and is given by the following relation: (see references (Angulo, *et al.*, 1999) and (Hosseinimotlagh and Shamsi, 2008).)

$$S(E) = S(0) + S'(0)E + S''(0)E^2 \quad (MeV - barn) \tag{26}$$

In the Table (8), the numerical values of $S(0)$, $S'(0)$ and $S''(0)$ from reference (Hosseinimotlagh and Shamsi, 2008) are given. Also, in the Table (9), the values of $S(E)$, $\sigma(E)$ and λ_f in $E = 0.01069682121$ (MeV) for above mentioned reactions are calculated which we will use them in this work. In the table (10) the numerical values of fusion rate are presented for MCF from reference (Angulo, *et al.*, 1999), (Pradler, 2009), (Hamaguchi, *et al.*, 2012) and (Fowler, *et al.*, 1967).

Another important point is ignoring the $^2H(d,\gamma)^4He$ branch in MCF, because the fusion rate of this branch is much smaller than other branches.

Table-8. The numerical values of $S(0)$, $S'(0)$ and $S''(0)$ ((Angulo, *et al.*, 1999) and (Fowler, *et al.*, 1967)

	$S(0)(MeV - barn)$	$S'(0)(MeV - barn)$	$S''(0)(MeV - barn)$
$^2H(d,n)^3He$	0.055	0.308	0.094
$^2H(d,p)^3H$	0.056	0.0204	0.0251
$^2H(d,\gamma)^4He$	56×10^{-10}	0.203×10^{-10}	few

Table–9. Our calculated numerical values of $S(E)$, $\sigma(E)$ and λ_f in $E = 0.01069682121$ (MeV) for SCF

$E = 0.01069682121$ (MeV)	$S(E)$ $(MeV - barn)$	$\sigma(E)$ $(barn)$	λ_f (s^{-1})
$^2H(d,n)^3He$	0.05828263049	1.107019594×10^5	$1.47523876 \times 10^{14}$
$^2H(d,p)^3H$	0.05621526300	1.067752040×10^5	$1.422909953 \times 10^{14}$
$^2H(d,\gamma)^4He$	$5.601183137 \times 10^{-9}$	$1.063486713 \times 10^{-2}$	1.417225883×10^7

Table-10. The calculated values of λ_f for MCF ((Alexander, *et al.*, 1990a) and (Alexander, *et al.*, 1990b))

i	Muon catalyzed fusion	λ_f^i (s^{-1})
1	$^2H(d,n)^3He$	1.1×10^{10}
2	$^2H(d,n)^3H$	1.1×10^{10}
3	$^2H(d,\gamma)^4He$	--------
4	$^3H(d,n)^4He$	6.9×10^{11}
5	$^3H(t,2n)^4He$	9.6×10^8

8. Point Kinetic Equations for $\tilde{\tau} - dd$ Fusion Cycle

Now, our main goal in this part is solving the point kinetic equations of $\tilde{\tau} - dd$ fusion cycle for three branch of fusion reactions that is listed in table (3) in order to calculate atomic and molecular

densities time variations within the reactor core. Finally, from our obtained results we can calculate the Stau cycle efficiency and energy gain.

Kinetic equations governing on the $\tilde{\tau} - dd$ fusion reactor core can be written as ([1and 23]):

$$\frac{dN_{\tilde{\tau}}(t)}{dt} = S_{\tilde{\tau}} - \lambda_a^{\tilde{\tau}d} C_d \varphi N_{\tilde{\tau}}(t) + (1-p_S^1)\lambda_f^1 N_{\tilde{\tau}dd}(t)$$

$$+(1-p_S^2-p_S^3)\lambda_f^2 N_{\tilde{\tau}dd}(t) + (1-p_S^4)\lambda_f^3 N_{\tilde{\tau}dd}(t) - \lambda_{\tilde{\tau}} N_{\tilde{\tau}}(t) \tag{27}$$

$$\frac{dN_d(t)}{dt} = -\lambda_a^{\tilde{\tau}d} C_d \varphi N_{\tilde{\tau}}(t) - \lambda_a^{\tilde{\tau}dd} C_d \varphi N_{\tilde{\tau}d}(t) + \lambda_{\tilde{\tau}} N_{\tilde{\tau}d}(t) \tag{28}$$

$$\frac{dN_{\tilde{\tau}d}(t)}{dt} = \lambda_a^{\tilde{\tau}d} C_d \varphi N_{\tilde{\tau}}(t) - \lambda_a^{\tilde{\tau}dd} C_d \varphi N_{\tilde{\tau}d}(t) - \lambda_{\tilde{\tau}} N_{\tilde{\tau}d}(t) \tag{29}$$

$$\frac{dN_{\tilde{\tau}dd}(t)}{dt} = \lambda_a^{\tilde{\tau}dd} C_d \varphi N_{\tilde{\tau}d}(t) - \lambda_f^1 N_{\tilde{\tau}dd}(t) - \lambda_f^2 N_{\tilde{\tau}dd}(t)$$

$$-\lambda_f^3 N_{\tilde{\tau}dd}(t) - \lambda_{\tilde{\tau}} N_{\tilde{\tau}dd}(t) \tag{30}$$

$$\frac{dN_{\tilde{\tau}^3He}(t)}{dt} = p_S^1 \lambda_f^1 N_{\tilde{\tau}dd}(t) - \lambda_{\tilde{\tau}} N_{\tilde{\tau}^3He}(t) \tag{31}$$

$$\frac{dN_{\tilde{\tau}t}(t)}{dt} = p_S^2 \lambda_f^2 N_{\tilde{\tau}dd}(t) - \lambda_{\tilde{\tau}} N_{\tilde{\tau}t}(t) \tag{32}$$

$$\frac{dN_{\tilde{\tau}p}(t)}{dt} = p_S^3 \lambda_f^2 N_{\tilde{\tau}dd}(t) - \lambda_{\tilde{\tau}} N_{\tilde{\tau}p}(t) \tag{33}$$

$$\frac{dN_{\tilde{\tau}^4He}(t)}{dt} = p_S^4 \lambda_f^3 N_{\tilde{\tau}dd}(t) - \lambda_{\tilde{\tau}} N_{\tilde{\tau}^4He}(t) \tag{34}$$

where, $S_{\tilde{\tau}} = 1 \ (cm^{-3})$ is the Stau injection rate into the liquid deuterium fuel, φ is the fraction of liquid hydrogen density , $N_{(i)}$ is the density of atoms and molecules inside the reactor core, i.e. $(i = \tilde{\tau}, d, \tilde{\tau}d, \tilde{\tau}^3He, \tilde{\tau}t, \tilde{\tau}^4He, \tilde{\tau}dd)$ .Parameters $\lambda_a^{\tilde{\tau}dd}$, $\lambda_m^{\tilde{\tau}dd}$, λ_f^i and p_S^i were introduced in the previous section. $\lambda_{\tilde{\tau}}$ is decay rate of Stau particle, as $\lambda_{\tilde{\tau}} = 1/\tau_{\tilde{\tau}} = \Gamma_{\tilde{\tau}}^{2-body}(\tilde{\tau} \to \tau + \tilde{G})$ and for Muon $\lambda_\mu = 1/\tau_\mu$. We solve these equations in both of steady state (time-independent density of atoms and molecules) and dynamical state (time-dependent density of atoms and molecules) with the use of computers (programming, Maple-15) and its results are presented in numerical section. Finally, to check the difference between densities in dynamical and steady states a new state is introduced ,that is called perturbation state. Also because the calculations in dynamics conditions are more precise and useful in comparing with static conditions, so we have been used the results of dynamics state condition for doing more work in the next sections. Also ,for comparing SCF with MCF, similarly, we solve above point kinetic equations for MCF with replacing the SCF parameters by MCF.we must be notice that the most important figures are the figuers of $\tilde{\tau}dd$ and μdd molecules density, because the result of these figures are used directly to calculate the fusion cycle efficiency, energy production and energy gain. For this reason we've presented only μdd molecule figures for the MCF.

9. Steady State Solution

To solve the above equations in steady state, we assume that:

$$\frac{dN_{\tilde{\tau}}(t)}{dt} = \frac{dN_{\tilde{\tau}d}(t)}{dt} = \frac{dN_{\tilde{\tau}dd}(t)}{dt} = \frac{dN_{\tilde{\tau}^3He}(t)}{dt} = \frac{dN_{\tilde{\tau}t}(t)}{dt}$$

$$= \frac{dN_{\tilde{\tau}p}(t)}{dt} = \frac{dN_{\tilde{\tau}^4He}(t)}{dt} = 0 \tag{35}$$

Thus we have:

$$\alpha_1 = \frac{\lambda_a^{\tilde{\tau}d} C_d \varphi}{\lambda_a^{\tilde{\tau}dd} C_d \varphi + \lambda_{\tilde{\tau}}} \tag{36}$$

$$\alpha_2 = \frac{\lambda_a^{\tilde{\tau}dd} C_d \varphi}{\lambda_f^1 + \lambda_f^2 + \lambda_f^3 + \lambda_{\tilde{\tau}}} \tag{37}$$

$$\alpha_3 = (1 - p_S^1)\lambda_f^1 N_{\tilde{\tau}dd} + (1 - p_S^2 - p_S^3)\lambda_f^2 N_{\tilde{\tau}dd} + (1 - p_S^4)\lambda_f^3 \tag{38}$$

$$N_{\tilde{\tau}dd}^* = \frac{S_{\tilde{\tau}}}{\dfrac{\lambda_a^{\tilde{\tau}d} C_d \varphi + \lambda_{\tilde{\tau}}}{\alpha_1 \alpha_2} - \alpha_3} \tag{39}$$

$$N_{\tilde{\tau}} = \frac{S_{\tilde{\tau}} + \alpha_3 N_{\tilde{\tau}dd}^*}{\lambda_a^{\tilde{\tau}d} C_d \varphi + \lambda_{\tilde{\tau}}} \tag{40}$$

$$N_{\tilde{\tau}d} = \frac{\lambda_a^{\tilde{\tau}d} C_d \varphi}{\lambda_a^{\tilde{\tau}dd} C_d \varphi + \lambda_{\tilde{\tau}}} \times \frac{S_{\tilde{\tau}} + \alpha_3 N_{\tilde{\tau}dd}^*}{\lambda_a^{\tilde{\tau}d} C_d \varphi + \lambda_{\tilde{\tau}}} \tag{41}$$

$$N_{\tilde{\tau}^3He} = \frac{p_S^1 \lambda_f^1 N_{\tilde{\tau}dd}^*}{\lambda_{\tilde{\tau}}} \tag{42}$$

$$N_{\tilde{\tau}t} = \frac{p_S^2 \lambda_f^2 N_{\tilde{\tau}dd}^*}{\lambda_{\tilde{\tau}}} \tag{43}$$

$$N_{\tilde{\tau}p} = \frac{p_S^3 \lambda_f^2 N_{\tilde{\tau}dd}^*}{\lambda_{\tilde{\tau}}} \tag{44}$$

$$N_{\tilde{\tau}^4He} = \frac{p_S^4 \lambda_f^3 N_{\tilde{\tau}dd}^*}{\lambda_{\tilde{\tau}}} \tag{45}$$

The results of this section are presented in the table (16) in numerical calculation section.

10. Dynamical State Solution

To solve the point kinetic energy in dynamical state, we get the atoms and molecules density over the time within the reactor core. In this case we see that the reactor reaches to steady state at the little time after power on and densities of production and consumption elements are constant or may change with uniform rate. Graphs and results of this section are presented in numerical calculation section.

11. Perturbation State

In this section, we considered the density difference between dynamical and steady state solution and call it a perturbation density:

$$N_{Perturbation} = \left| N_{Steady\ state} - N_{Dynamic} \right| \tag{46}$$

The results of this section are presented in table (16) in numerical calculation section.

12. Stau Cycle Efficiency and Energy Gain

We show the Stau cycle efficiency with $\chi_{\tilde{\tau}}$, which represents the average number of times that a Stau (or Muon) repeated the fusion cycle and is calculated from the following equation ((Harms, *et al*, 2002) and (Hosseinimotlagh, and Shamsi, 2008)):

$$\chi_{\tilde{\tau}} = \sum_{i=1}^{3} \chi_{\tilde{\tau}}^{i} = \sum_{i=1}^{3} \left(\int_{0}^{t_{\tilde{\tau}}+T} \lambda_f^i N_{\tilde{\tau}dd}(t)dt \Big/ \int_0^T S_{\tilde{\tau}}dt \right) \approx \sum_{i=1}^{3} \lambda_f^i N_{\tilde{\tau}dd}^* \times t_{\tilde{\tau}} \tag{47}$$

As mentioned before, $S_{\tilde{\tau}} = 1 \ (cm^{-3})$ is the rate of Stau injection rate into the liquid deuterium fuel and T is the reactor operating time. $N_{\tilde{\tau}dd}^*$ is Stau deuterium-deuterium molecule density in reactor core when it was achieved steady state and its value is obtained from the above point kinetic equations for Stau and Muon. The numerical calculated values of Stau and Muon efficiency and energy production are presented in the steady and dynamical state in tables (11) and (12).

Table-11. The calculated values of Stau cycle efficiency in the different state for $\varphi = 1$.

i	reaction	Stau cycle efficiency for deuterium fuel		
		condition		
		Static	dynamic	perturbation
1	$^2H(d,n)^3He$	1.3384×10^8	1.3384×10^8	0.0000
2	$^2H(d,n)^3H$	1.2910×10^8	1.2909×10^8	1.0000×10^4
3	$^2H(d,\gamma)^4He$	1.2858×10^1	1.2858×10^1	0.0000
Total		2.6294×10^8	2.6293×10^8	1.0000×10^4

Table-12. The calculated values of Muon cycle efficiency in the different state for $\varphi = 1$.

i	reaction	Muon cycle efficiency for deuterium fuel		
		condition		
		static	dynamic	perturbation
1	$^2H(d,n)^3He$	123.456	122.200	1.256
2	$^2H(d,n)^3H$	123.456	122.200	1.256
3	$^2H(d,\gamma)^4He$	few	few	few
Total		246.912	244.400	2.512

Now we will calculate the energy gain with regard to Stau and Muon production methods which discussed in pervious section.

Energy gain from the following equation is obtained ((Harms, *et al*, 2002) and (Hosseinimotlagh, and Shamsi, 2008)).

$$G = \frac{\sum_{i=1}^{3} Q_i \chi_{\tilde{\tau}}^i}{E_{\tilde{\tau}}} \tag{48}$$

Where Q_{dd_i} is energy produced from each of the *dd* fusion branch which was previously mentioned. $E_{\tilde{\tau}}$ is the energy required to produce one Stau that was previously calculated. Also the energy required to produce one Muon is about $4000(MeV)$. The energy gain for different states in tables (13) to (16) are presented.

Table-13. The calculated values of energy produced for injection one Stau for $\varphi = 1$.

	Values of Energy production for deuterium fuel (MeV)	
i	reaction	condition

		static	dynamic	perturbation
1	$^2H(d,n)^3He$	4.2090×10^8	4.2088×10^8	2.0000×10^4
2	$^2H(d,n)^3H$	5.0368×10^8	5.0367×10^8	1.0000×10^4
3	$^2H(d,\gamma)^4He$	2.9664×10^2	2.9664×10^2	0.0000
Total		9.2458×10^8	9.2455×10^8	3.0000×10^4

Table-14. The calculated values of energy produced for injection one Muon for $\varphi=1$.

		Values of Energy production for deuterium fuel		(MeV)
i	reaction	condition		
		static	dynamic	perturbation
1	$^2H(d,n)^3He$	388.2222	384.2701	3.9521
2	$^2H(d,n)^3H$	481.6666	476.7633	4.9033
3	$^2H(d,\gamma)^4He$	few	few	few
Total		869.8888	861.0334	8.8554

Table-15. The calculated values of energy gain for injection one Stau for $\varphi=1$.

		Energy gain for deuterium fuel		
i	reaction	condition		
		static	dynamic	perturbation
1	$^2H(d,n)^3He$	4.2090×10^{-9}	4.2088×10^{-9}	2.0000×10^{-13}
2	$^2H(d,n)^3H$	5.0368×10^{-9}	5.0367×10^{-9}	1.0000×10^{-13}
3	$^2H(d,\gamma)^4He$	2.9664×10^{-15}	2.9664×10^{-15}	0.0000
Total		9.2458×10^{-9}	9.2455×10^{-9}	3.0000×10^{-13}

Table-16. The calculated values of energy gain for injection one Muon for $\varphi=1$.

		Energy gain for deuterium fuel		
i	reaction	condition		
		static	dynamic	perturbation
1	$^2H(d,n)^3He$	0.09705	0.09667	9.8802×10^{-4}
2	$^2H(d,n)^3H$	0.1242	0.1191	1.2258×10^{-3}
3	$^2H(d,\gamma)^4He$	few	few	Few
Total		0.2117	0.2152	2.2138×10^{-3}

13. Fusion Reaction Rate and Power Density

To calculate the fusion reaction rate and power density we need to calculate the average value of $\langle\sigma v\rangle$,therefore we use of below equation(15) .Where

$$\sigma = \frac{S(E)}{E}\exp\left(-\sqrt{\frac{E_G}{E}}\right) \tag{49}$$

E_G is Gamow energy:

$$E_G = (2\pi\alpha Z_0 Z_1)^2(Mc^2/2) \tag{50}$$

$$S(E) = S(0)\left(1 + \frac{S'(0)}{S(0)}E + \frac{1}{2}\frac{S''(0)}{S(0)}E^2\right) \tag{51}$$

Now put these relations in equation (15) and multiply it in $c = 2.99792458 \times 10^{10}$ (cm/s) (due to unit conversion) we have:

$$\langle \sigma v \rangle = c \times \frac{(8/\pi)^{1/2}}{M^{1/2}(kT)^{3/2}} \int S(E) \exp\left(-\frac{E_G^{1/2}}{E^{1/2}} - \frac{E}{kT}\right) dE$$

$$= c \left(\frac{2}{M}\right)^{1/2} \frac{\Delta E_0}{(kT)^{3/2}} S_{eff} \exp(-\tau) \qquad (cm^3/s) \qquad (52)$$

In this relation, S_{eff} is effective spectroscopic factor which can be written as:

$$S_{eff} = S(0)[1 + \frac{5}{12\tau} + \frac{S'(0)}{S(0)}\left(E_0 + \frac{35}{36}kT\right)$$

$$+ \frac{1}{2}\frac{S''(0)}{S(0)}\left(E_0^2 + \frac{89}{36}E_0 kT\right)\}] \qquad (MeV - barn) \qquad (53)$$

Also M and A are reduced mass and reduced atomic number, respectively. Parameters W, E_0, τ and ΔE_0 are defined as :

$$M = m_0 m_1 / m_0 + m_1 \qquad (54)$$

$$A = A_0 A_1 / A_0 + A_1 \qquad (55)$$

$$W = Z_0^2 Z_1^2 A \qquad (56)$$

$$E_0 = \left[\pi \alpha Z_0 Z_1 kT (Mc^2/2)\right]^{2/3} = 0.122041933 \ W^{1/3} \ T_9^{2/3} \quad (MeV) \qquad (57)$$

$$\tau = \frac{3E_0}{kT} = 4.248708782 \quad (MeV) \qquad (58)$$

$$\Delta E_0 = 4 \times \left(\frac{E_0 kT}{3}\right)^{1/2} = 0.2368321120 \ W^{1/2} \ T_9^{5/6} \quad (MeV) \qquad (59)$$

And inserting these relations inside to the equation (53) finally S_{eff} is given by the following relation:

$$S_{eff} = S(0)[\ 1 + 0.09806901063 \ W^{-1/3}T_9^{1/3}$$

$$+ \frac{S'(0)}{S(0)}\left(0.122041933 \ W^{1/3}T_9^{2/3} + 0.08377972158 \ T_9\right)$$

$$+ \frac{S''(0)}{S(0)}\left(0.007447116705 \ W^{2/3}T_9^{4/3} + 0.01299989837 \ W^{1/3}T_9^{5/3}\right)\ ](MeV - barn) \ (60)$$

We have calculated $\langle \sigma v \rangle$ for different amounts of energy and our calculated results are presented in Table (17).

Now we can calculate the fusion reaction rate by using the following equation (Harms, *et al*, 2002):

$$R_{fu} = N_a N_b \langle \sigma v \rangle \quad (reaction/cm^3) \qquad (61)$$

Where, N_a and N_b are the densities of reactive particles. If the fuel is composed of only one type of particle (here we have only deuterium), then this equation becomes the following form:

$$R_{fu} = \frac{N^2}{2}\langle \sigma v \rangle \quad (reaction/cm^3) \qquad (62)$$

In this article

$$N = N_d = 4.25 \times 10^{22} \ atoms/cm^3 \qquad (63)$$

Also fusion power density can be calculated as below:

$$P_{fu} = R_{fu}Q_{fu} \quad (MeV/s \ cm^3) \qquad (64)$$

Where Q_{fu} is the fusion energy .Now we must be entered the fraction of reaction branch in equation (61). Thus we have:

$$P_{fu} = \frac{N_d}{2} \sum_{i=1}^{3} \frac{\chi_{\tilde{\tau}}^i}{\chi_{\tilde{\tau}}} Q_{fu}^i \langle \sigma v \rangle^i \quad (MeV/s\ cm^3) \tag{65}$$

$\chi_{\tilde{\tau}}^i / \chi_{\tilde{\tau}}$ is the average fraction of each reaction branch.

However, we must notice that which deuterium density inside the reactor core is reduced over time (and subsequently reduced the formation rates of $\tilde{\tau}d$ and $\tilde{\tau}dd$). Finally for fusion power density we have:

$$P_{fu}(t) = R_{fu}(t)Q_{fu} \ \square \ \frac{N_d^2(t)}{2} \sum_{i=1}^{3} \frac{\chi_{\tilde{\tau}}^i}{\chi_{\tilde{\tau}}} Q_{fu}^i \langle \sigma v \rangle^i \quad (MeV/s\ cm^3) \tag{66}$$

We calculated deuterium injection rate into the reactor core (for constant fuel density and reactor power) in the dynamical state. You can clearly see that from Figure (4) which in the interval $10^{-10} \leq \varphi \leq 1$, the rate of deuterium density has a linear and uniform shape, and so:

$$R_d = \frac{dN_d}{dt} \ \square \ \frac{5.254 \times 10^8}{2.776233891 \times 10^7} = 18.9249 \quad (\#/cm^3\ s) \tag{67}$$

Where, R_d is burning rate (also, deuterium burning and injection rate can be calculated using the Stau cycle coefficient).

Therefore, the time-dependent density of deuterium is:

$$N_d(t) = N_d - (R_d \times t) \quad (\#/cm^3) \tag{68}$$

And finally, the time-dependent reaction power density is:

$$P_{fu}(t) = \frac{(N_d - (R_d \times t))^2}{2} \sum_{i=1}^{3} \frac{\chi_{\tilde{\tau}}^i}{\chi_{\tilde{\tau}}} Q_{fu}^i \langle \sigma v \rangle^i \quad (MeV/s\ cm^3) \tag{69}$$

Note that, for the interval $0 \leq \varphi \leq 10^{-10}$, the fusion power density are reduced because all parameters depend on the deuterium density (such as atomic and molecular formation rates), so the reactor does not reach steady state in this interval.

14. Numerical Calculations

In this section we use from the numerical values in the previous section and using tables (5) to (10) for solving point kinetic equations in terms of time for SCF and MCF . (see figures 4 to 8)

The reader must be notice that all calculations are performed for SCF under conditions $S_{\tilde{\tau}} = 1\ (cm^{-3})$ and at time $t = \tau_{\tilde{\tau}} = 2.776233891 \times 10^7$ and similarly for the MCF under choosing $S_{\mu} = 1\ (cm^{-3})$ and at time $t = 3600(\text{sec})$. For MCF, we have assumed that at time $t = 3600(\text{sec})$ continuous injections of Muon in the reactor core were performed, S_{μ} are kept constant to reach steady state.

Figure-4. Variations of deuterium density in terms of time and liquid hydrogen density a) in the range $0 \leq \varphi \leq 10^{-10}$ and b) $0 \leq \varphi \leq 1$.
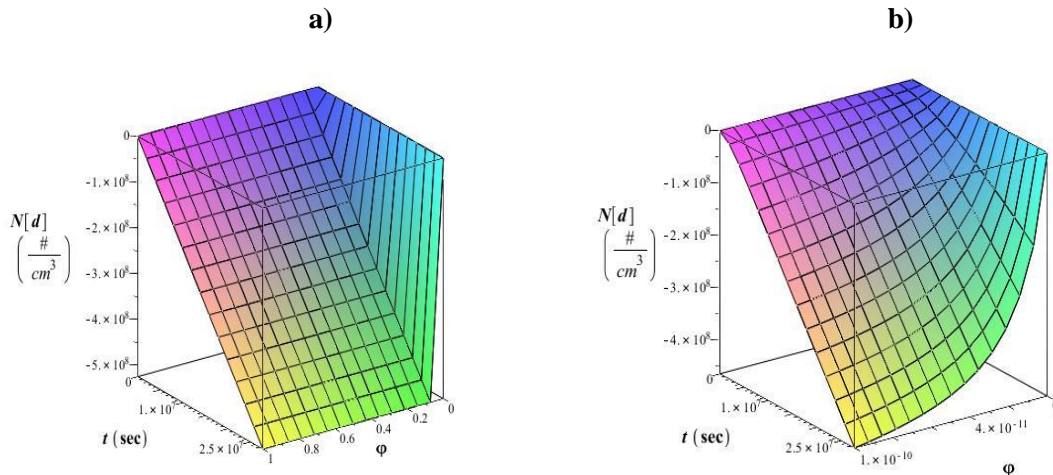
a)   **b)**

Figure.4 shows that, since we have no consider the fuel injection in the system during the process, the deuterium density is reduced versus time (the numerical values inside the graphs indicate that the deuterium burning), this point it is obvious from equation (28). Also you can see that if deuterium density fraction is less than 10^{-10}, variations in the density of deuterium have not a regular rate. This is due to the low density of deuterium in the reaction and reduce it over time. Thus the formations rates of $\tilde{\tau}d$ and $\tilde{\tau}dd$ are reduced, and subsequently the Stau cycle efficiency and energy gain are reduced. So in this case the reactor cannot reach to steady state. But in the interval $10^{-10} \leq \varphi \leq 1$, variations of deuterium density over time have a uniform rate.

Figure-5. Variations of $\tilde{\tau}dd$ molecular density in terms of time and liquid hydrogen density a)in the range $0 \leq \varphi \leq 10^{-10}$ and b) $0 \leq \varphi \leq 1$.

a)   b)
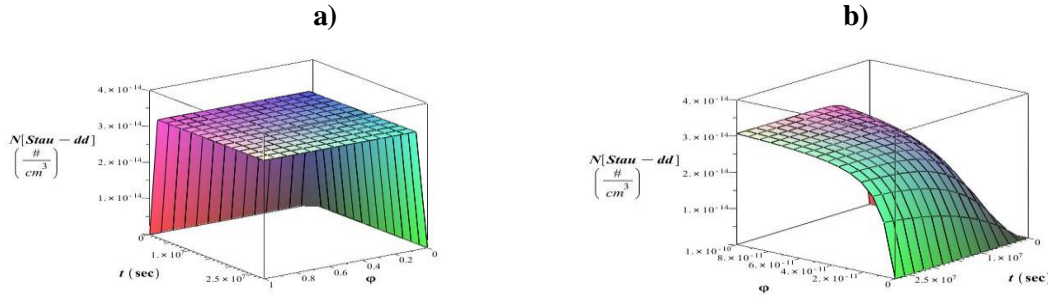
From figure.5 we see clearly that, in the interval $10^{-10} \leq \varphi \leq 1$, $\tilde{\tau}dd$ molecule density reaches a constant value $N_{\tilde{\tau}dd} = N_{\tilde{\tau}dd}^{*} = 3.2680 \times 10^{-14}$ which indicates the status of the reactor is in steady state. Also we see that the time required to reach steady state is very small.

Figure-6. Variations of a) $\tilde{\tau}d$ atom density and b) $\tilde{\tau}$ particle density in terms of time and liquid hydrogen density in the range of $0 \leq \varphi \leq 1$.

a)   b)
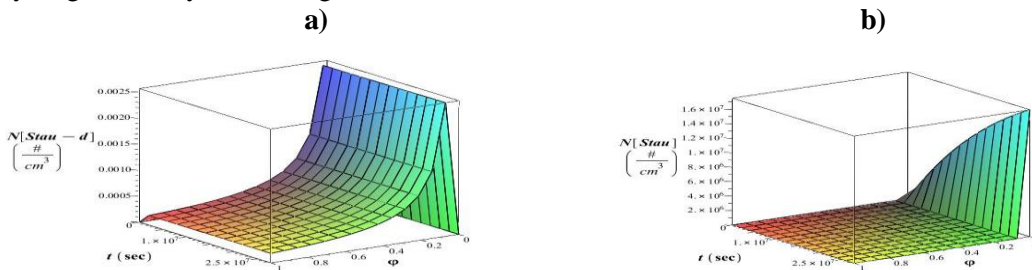
From figure .6 we see clearly that ,after the reactor to reach steady state Stau density is almost zero, that is why Stau quickly reacts with the fuel or stick to the one of the charged particles resulting from the reaction. Similarly, this issue is obvious for the $\tilde{\tau}d$ density changes and figures of Stau sticking to the charged particles.

Figure-7. Variations of a) $\tilde{\tau}^{3}He$,b) $\tilde{\tau}t$,c) $\tilde{\tau}p$ and d) $\tilde{\tau}^{4}He$ atom densities in terms of time and liquid hydrogen density in the range of $0 \leq \varphi \leq 1$

a)   b)

c)

d)
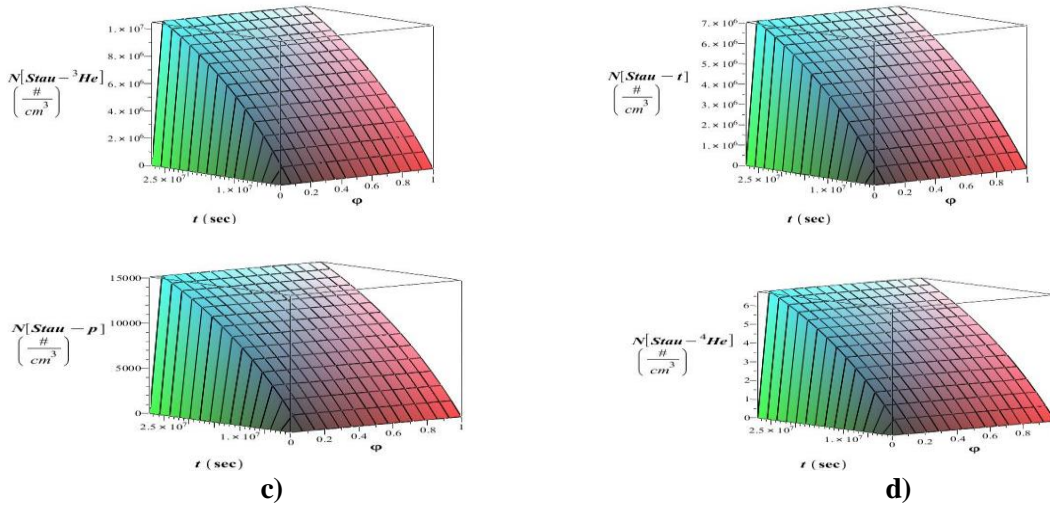
As you can see that from figure.7 the relation $N_{\tilde{\tau}^4He} < N_{\tilde{\tau}p} < N_{\tilde{\tau}t} < N_{\tilde{\tau}^3He}$ between them is dominant. This relationship shows that the production rate of $\tilde{\tau}^3He$ is more than $\tilde{\tau}t$ and $\tilde{\tau}p$ because the Stau sticking coefficient to ^3He is greater than t and p .

But in the case of $\tilde{\tau}^4He$, although the Stau sticking coefficient to ^4He more than ^3He , therefore we must be notice that the fusion probability of the branch $^2H(d,n)^3He$ is much greater than $^2H(d,\gamma)^4He$. For having a comparison between Stau catalyzed dd fusion with muon catalyzed dd fusion we have plotted figure .8.

Figure-8. Variations of μdd molecular density in terms of time and liquid hydrogen density a)in the range $0 \le \varphi \le 1$ and b) $10^{-7} \le \varphi \le 1$.

a)   **b)**
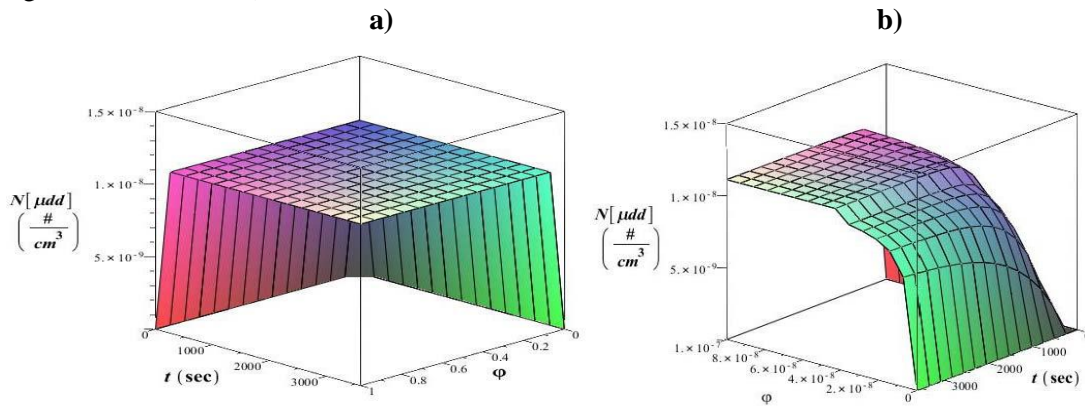
From this figure you can see that in the interval $10^{-7} \le \varphi \le 1$, $\tilde{\tau}dd$ molecule density reaches a constant value $N_{\mu dd} = N^*_{\mu dd} = 1.111 \times 10^{-8}$ which indicates the status of the reactor is in steady state. Also we see that the time required to reach steady state is very small.

15. Conclusion

As we saw in this article, Stau catalyzed fusion (SCF) can be produced energy about $9.2455 \times 10^8 (MeV)$ and it compared with Muon catalyzed fusion (MCF) which produced energy about $10^3 (MeV)$ is very impressive. This value, even in comparison with the fission reaction rate is very large. For example, the nucleus of Uranium-235 is only about $200(MeV)$ of energy generated. But the most important problem in the way is the high cost of Stau production, and as we saw in the

previous sections the obtained energy gain is less than one for SCF. But we must be notice that supersymmetry is a new theory, and our knowledge about the supersymmetric particles and methods of its production is very low. We hope that low cost methods to produce these particles can be found. Another point is that, because almost all supersymmetric particles will decay quickly to Stau, so most likely access to inexpensive method for producing Stau will increaseAlso,in future we can likely to be able to put the targets inside the space stations and spacecraft body to produce Stau by using cosmic rays (Ahlers, *et al.*, 2007).We hope that Stau catalyzed fusion become economical method to produce energy in the future.

Table-16. The numerical calculated values of the density of $\tilde{\tau}dd$ and μdd molecules in terms of the different values of fuel fraction density per one catalyst particle injection rate . These values are obtained from solving kinetic equations (27) to (34) in steady and dynamical state. Also the perturbation values between these states are calculated.

	Stau catalyzed fusion			Muon catalyzed fusion		
	$N^{*}_{\tilde{\tau}dd}$ $(\#/cm^3)$			$N^{*}_{\mu dd}$ $(\#/cm^3)$		
φ	Steady state	Dynamical state	Perturbation	Steady state	Dynamical state	Perturbation
0.05	1.8060×10^{-16}	3.2680×10^{-14}	3.2499×10^{-14}	2.3918×10^{-12}	1.1100×10^{-8}	1.1098×10^{-8}
0.10	3.7894×10^{-16}	3.2680×10^{-14}	3.2301×10^{-14}	5.0482×10^{-12}	1.1100×10^{-8}	1.1095×10^{-8}
0.15	5.9777×10^{-16}	3.2680×10^{-14}	3.2082×10^{-14}	8.0157×10^{-12}	1.1100×10^{-8}	1.1092×10^{-8}
0.20	8.4044×10^{-16}	3.2680×10^{-14}	3.1839×10^{-14}	1.1352×10^{-11}	1.1100×10^{-8}	1.1099×10^{-8}
0.25	1.1111×10^{-15}	3.2680×10^{-14}	3.1568×10^{-14}	1.5131×10^{-11}	1.1100×10^{-8}	1.1085×10^{-8}
0.30	1.4148×10^{-15}	3.2680×10^{-14}	3.1265×10^{-14}	1.9447×10^{-11}	1.1100×10^{-8}	1.1080×10^{-8}
0.35	1.7580×10^{-15}	3.2680×10^{-14}	3.0922×10^{-14}	2.4422×10^{-11}	1.1100×10^{-8}	1.1076×10^{-8}
0.40	2.1490×10^{-15}	3.2680×10^{-14}	3.0531×10^{-14}	3.0221×10^{-11}	1.1100×10^{-8}	1.1070×10^{-8}
0.45	2.5986×10^{-15}	3.2680×10^{-14}	3.0081×10^{-14}	3.7067×10^{-11}	1.1100×10^{-8}	1.1063×10^{-8}
0.50	3.1210×10^{-15}	3.2680×10^{-14}	2.9559×10^{-14}	4.5271×10^{-11}	1.1100×10^{-8}	1.1055×10^{-8}
0.55	3.7352×10^{-15}	3.2680×10^{-14}	2.8944×10^{-14}	5.5282×10^{-11}	1.1100×10^{-8}	1.1045×10^{-8}
0.60	4.4681×10^{-15}	3.2680×10^{-14}	2.8211×10^{-14}	6.7770×10^{-11}	1.1100×10^{-8}	1.1032×10^{-8}
0.65	5.3575×10^{-15}	3.2680×10^{-14}	2.7322×10^{-14}	8.3785×10^{-11}	1.1100×10^{-8}	1.1016×10^{-8}
0.70	6.4597×10^{-15}	3.2680×10^{-14}	2.6220×10^{-14}	1.0507×10^{-10}	1.1100×10^{-8}	1.0995×10^{-8}
0.75	7.8614×10^{-15}	3.2680×10^{-14}	2.4818×10^{-14}	1.3473×10^{-10}	1.1100×10^{-8}	1.0965×10^{-8}
0.80	9.7038×10^{-15}	3.2680×10^{-14}	2.2976×10^{-14}	1.7892×10^{-10}	1.1100×10^{-8}	1.0921×10^{-8}
0.85	1.2233×10^{-14}	3.2680×10^{-14}	2.0447×10^{-14}	2.5180×10^{-10}	1.1100×10^{-8}	1.0848×10^{-8}
0.90	$1.5923\times10^{-}$	$3.2680\times10^{-}$	1.6757×10^{-14}	$3.9470\times10^{-}$	$1.1100\times10^{-}$	1.0705×10^{-8}

0.95	2.1809×10^{-14}	3.2680×10^{-14}	1.0871×10^{-14}	8.0193×10^{-10}	1.1100×10^{-8}	1.0298×10^{-8}
1.00	3.2681×10^{-14}	3.2680×10^{-14}	1.0000×10^{-18}	1.1223×10^{-8}	1.1100×10^{-8}	1.2300×10^{-10}

Table-17. The numerical calculated values of $\langle \sigma v \rangle$ in terms of E for different fusion reactions.

E (MeV)	$\langle \sigma v \rangle \quad (cm^3/s)$		
	$^2H(d,n)^3He$	$^2H(d,p)^3H$	$^2H(d,\gamma)^4He$
0.001	$1.003767767 \times 10^{-22}$	$1.008420159 \times 10^{-22}$	$1.056027303 \times 10^{-25}$
0.002	$3.154222654 \times 10^{-21}$	$3.143519692 \times 10^{-21}$	$3.222231897 \times 10^{-24}$
0.003	$1.627728600 \times 10^{-20}$	$1.611401600 \times 10^{-20}$	$1.623273675 \times 10^{-23}$
0.004	$4.522429468 \times 10^{-20}$	$4.450740864 \times 10^{-20}$	$4.415653320 \times 10^{-23}$
0.005	$9.289154704 \times 10^{-20}$	$9.093121535 \times 10^{-20}$	$8.897316620 \times 10^{-23}$
0.006	$1.601694368 \times 10^{-19}$	$1.560175649 \times 10^{-19}$	$1.507113846 \times 10^{-22}$
0.007	$2.467925391 \times 10^{-19}$	$2.392918367 \times 10^{-19}$	$2.283865174 \times 10^{-22}$
0.008	$3.518874812 \times 10^{-19}$	$3.397207926 \times 10^{-19}$	$3.205623315 \times 10^{-22}$
0.009	$4.742935815 \times 10^{-19}$	$4.560271042 \times 10^{-19}$	$4.256575496 \times 10^{-22}$
0.010	$6.127440912 \times 10^{-19}$	$5.868630827 \times 10^{-19}$	$5.421048445 \times 10^{-22}$
0.020	$2.633832152 \times 10^{-18}$	$2.445025433 \times 10^{-18}$	$2.068320360 \times 10^{-21}$
0.030	$5.301827721 \times 10^{-18}$	$4.810103434 \times 10^{-18}$	$3.790474342 \times 10^{-21}$
0.040	$8.241144715 \times 10^{-18}$	$7.342152700 \times 10^{-18}$	$5.442729644 \times 10^{-21}$
0.050	$1.129152769 \times 10^{-17}$	$9.910358509 \times 10^{-18}$	$6.957499472 \times 10^{-21}$
0.060	$1.437685982 \times 10^{-17}$	$1.245990120 \times 10^{-17}$	$8.325970793 \times 10^{-21}$
0.070	$1.745805959 \times 10^{-17}$	$1.496696814 \times 10^{-17}$	$9.557369050 \times 10^{-21}$
0.080	$2.051408085 \times 10^{-17}$	$1.742160214 \times 10^{-17}$	$1.066576001 \times 10^{-20}$
0.090	$2.353334872 \times 10^{-17}$	$1.982041670 \times 10^{-17}$	$1.166552904 \times 10^{-20}$
0.100	$2.650954937 \times 10^{-17}$	$2.216324126 \times 10^{-17}$	$1.256987735 \times 10^{-20}$
0.200	$5.370867734 \times 10^{-17}$	$4.297474797 \times 10^{-17}$	$1.827908007 \times 10^{-20}$
0.300	$7.689894029 \times 10^{-17}$	$6.039554014 \times 10^{-17}$	$2.095931512 \times 10^{-20}$
0.400	$9.707075818 \times 10^{-16}$	$7.561286043 \times 10^{-17}$	$2.238127269 \times 10^{-20}$

0.500	$1.148943772\times10^{-16}$	$8.924378557\times10^{-17}$	$2.317207431\times10^{-20}$
0.600	$1.308191325\times10^{-16}$	$1.016527986\times10^{-16}$	$2.317207431\times10^{-20}$
0.700	$1.451623067\times10^{-16}$	$1.130776230\times10^{-16}$	$2.383181997\times10^{-20}$
0.800	$1.581582587\times10^{-16}$	$1.236844424\times10^{-16}$	$2.391944768\times10^{-20}$
0.900	$1.699863806\times10^{-16}$	$1.335954123\times10^{-16}$	$2.391820989\times10^{-20}$
1.000	$1.807879339\times10^{-16}$	$1.429037843\times10^{-16}$	$2.385726998\times10^{-20}$

References

Ahlers, M., Kersten, J. and Ringwald, A., (2006). Long-lived staus at neutrino telescopes. arXiv:hep-ph/0604188v2.

Ahlers, M. et al., (2007). Long-lived staus from cosmic rays. arXiv:0705.3782v1 [hep-ph].

Alexander,S. A., Froelich, P. and Monkhorst, H. J., (1990). Nuclear fusion rates of muonic molecular ions. Physics Review A., 41(5): 2854-2857.

Aitchison, Ian. J. R., (2007). Supersymmetry in particle physics: Cambridge University press.

Alexander,S. A., Froelich, P. and Monkhorst, H. J., (1990). Nuclear fusion rates of muonic molecular ions. Physics Review A., 43(5): 2585.

Angulo, C. et al., (1999). A complication of charged-particle induced thermonuclear reaction rates. Nuclear Physics A., 656(1): 3-183.

Brandenburg, A. et al., (2005). Signatures of axinos and gravitinos at colliders. ArXiv:hep-ph/0501287v2.

Buchmuller, W. et al., (2004). Gravitino and goldstino at colliders. ArXiv:hep-ph/0403203v1.

Buchmuller, W. et al., (2004). Supergravity at colliders. arXiv:hep-ph/0402179v2.

Cripps, G. R., (1993). Interactive muon catalyzed and intertial confinement fusion. McMaster University, (Thesis-Ph.D), Availible from http://digitalcommons.mcmaster.ca/opendissertations/2721.

Delphi, Collaboration., (2001). Search for supersymmetric particles in scenarios with a gravitino LSP and stau NLSP. arXiv:hep-ex/0103026v1.

Desch, K., Fleischmann, S. and Wienemann, P., (2011). Stau as the lightest supersymmetric particle in r-parity violating Susy models: Discovery potential with early LHC data. arXiv:1008.1580v3 [hep-ph].

Dreiner, H. et al., (2010). Testing the CP-violating MSSM in Stau decays at the LHC and ILC. arXiv:1011.2449v1 [hep-ph].

Eidelman, S. et al., (2004). Review of particle physics. Phys. Lett. B, 592: 1.

Feng, J. L. and Smith, B. T., (2005). Slepton trapping at the large hadron and international linear colliders.

Fowler, W. et al., (1967). Thermonuclear reaction rates. Annual Review of Astronomy and Astrophysics, 5: 525-570.

Hamaguchi, K. et al., (2004). A study of late decaying charged particles at future colliders. arXiv:hep-ph/0409248v2.

Hamaguchi, K., Nojiri, M. and Roeck, A. D., (2006). Prospects to study a long-lived charged next lightest supersymmetric particle at the LHC. arXiv:hep-ph/0612060v1.

Hamaguchi, K. et al., (2012). Stau-catalyzed d-t nuclear fusion. arXiv:1202.2669v1 [hep-ph].

Harms, A. A., Miley, G. H. and Kingdon, D. R., (2002). Principles of fusion energy. Word Scientific.

Heckman, J. J., Jing, Shao. and Cumrun, Vafa., (2010). F-theory and the LHC: Stau search. arXiv:1001.4084v2 [hep-ph].

Hosseinimotlagh, S.N. and Shamsi, R., (2008). Determination of total average number of dd fusion in stau cycle in stau-catalyzed dd nuclear fusion in steady state condition. Infinite Energy, (80).

Loff, B. L. et al., (1981). Heavy stable particles and cold catalysis of nuclear fusion. Acta Physica Polonica, B12(3): 229- 235.

Martin, S. P., (2008). A supersymmetry primer. arXiv:hep-ph/9709356v5.

Panotopoulos, G., (2008). Supersymmetric dark matter, catalyzed BBN, and heavy moduli in MSUGRA with gravitino LSP and stau NLSP. arXiv:0812.3987v1 [hep-ph].

Pradler, J., (2009). The long-lived stau as a thermal relic. arXiv:0909.3429v1 [hep-ph].

Porod,W., (1998). Phenomenology of stops, sbottoms, staus and tau-sneutrino. arXiv:hep-ph/9804208v1.

Roeck, A. De. et al., (2005). Supersymmetric benchmarks with non-universal scalar masses or gravitino dark matter. arXiv:hep-ph/0508198v1.